Near-Infrared-Emitting Heteroleptic Cationic Iridium Complexes Derived from 2,3-Diphenylbenzo[*g*]quinoxaline as In Vitro Theranostic Photodynamic Therapy Agents

Li Wang,[a] Huimin Yin,[b] Peng Cui,[a,c] Marc Hetu,[b] Chengzhe Wang,[a] Susan Monro,[b] Richard Schaller,[d] Colin G. Cameron,[e] Bingqing Liu,[a] Svetlana Kilina,[a] Sherri A. McFarland*,[b,e] and Wenfang Sun*,[a]

[a] Department of Chemistry and Biochemistry, North Dakota State University, Fargo, North Dakota 58108-6050, United States

[b] Department of Chemistry, Acadia University, 6 University Avenue, Wolfville, NS B4P 2R6, Canada

[c] Materials and Nanotechnology Program, North Dakota State University, Fargo, North Dakota 58108-6050, United States

[d] Center for Nanoscale Materials, Argonne National Laboratory, Argonne, IL 60439, United States

[e] Department of Chemistry and Biochemistry, University of North Carolina at Greensboro, 310 McIver Street, Greensboro, NC 27402-6170, United States

Experimental Details

Cell culture

SK-MEL-28. Adherent SK-MEL-28 malignant melanoma cells (ATCC HTB-72) were cultured in Eagle's Minimum Essential Medium (EMEM, Mediatech Media MT-10 009-CV) supplemented with 10% FBS and were incubated at 37 °C under 5% CO2 and passaged 2-3 times per week according to standard aseptic procedures. SK-MEL-28 cells were started at 200,000 cells/mL in 75 cm2 tissue culture flasks and were subcultured when growth reached 550,000 cells/mL by removing old culture media and rinsing the cell layer once with Dulbecco's phosphate buffered saline (DPBS 1X, Mediatech, 21-031-CV), followed by dissociation of cell monolayer with 1X Trypsin-EDTA solution (0.25% (w/v Trypsin/0.53 mM EDTA, ATCC 30-2101). Complete growth medium was added to the cell suspension to allow appropriate aliquots of cells to be transferred to new cell vessels. Complete media was prepared in 150-mL portions as needed by combing EMEM (135 mL) and FBS (15 mL, prealiquoted and heat inactivated) in a 250-mL Millipore vacuum stericup (0.22 μm) and filtering.

CCD-1064Sk. Adherent CCD-1064SK normal skin fibroblasts (ATCC CRL-2076) were cultured in Iscove's Modified Dulbecco's Medium (IMDM) supplemented with 10% FBS (PAA Laboratories, A15-701), were incubated at 37 °C under 5% CO2, and were passaged 2−3 times per week according to standard aseptic procedures. CCD-1064SK cells were started at 200,000 cells mL^{-1} in 75 cm^2 tissue culture flasks and were subcultured when growth reached 550,000 cells mL^{-1} by removing old culture medium and rinsing the cell monolayer once with Dulbecco's phosphate buffered saline (DPBS 1X, Mediatech, 21-031-CV), followed by dissociation of the cell monolayer with trypsin-EDTA solution (0.25% w/v Trypsin/0.53 mM EDTA, ATCC 30-2101). Complete growth medium was added to the cell suspension to allow appropriate aliquots of cells to be transferred to new cell vessels. Complete growth medium was prepared in 150 mL portions as needed by combining IMDM (225 mL) and FBS (25 mL, prealiquoted and heat inactivated) in a 250 mL Millipore vacuum stericup (0.22 μm) and filtering.

Cytotoxicity and photocytotoxicity. Stock solutions of the iridium complexes were prepared at 5 mM in 10% DMSO in water and kept at -20 °C prior to use. Working dilutions were made by diluting the aqueous stock with pH 7.4 Dulbecco's phosphate buffered saline (DPBS). DPBS is a balanced salt solution of 1.47 mM potassium phosphate monobasic, 8.10 mM sodium phosphate dibasic, 2.68 mM potassium chloride, and 0.137 M sodium chloride. DMSO was kept at 1% or less in all of the final assay wells.

Cell viability experiments were performed in triplicate in 96-well ultra-low attachment flat bottom microtiter plates (Corning Costar, Acton, MA), where outer wells along the periphery contained 200 μL DPBS (2.68 mM potassium chloride, 1.47 mM potassium phosphate monobasic, 0.137 M sodium chloride, and 8.10 mM sodium phosphate dibasic) to minimize evaporation from sample wells. SK-MEL-28 cells growing in log phase (~550,000-600,000 cells mL^{-1}) with at least 93% viability were transferred in 50-μL aliquots to inner wells containing warm culture medium (25 μL) and placed in a 37 °C, 5% CO2 water-jacketed incubator (Thermo Electron Corp., FormaSeries II, Model 3110, HEPA Class 100) for 3 h to equilibrate (and allow for efficient cell attachment). Metal compounds were serially diluted with DPBS and pre-warmed at 37 °C before 25 μL aliquots of the appropriate dilutions were added to cells. Complexes-treated microplates were incubated at 37 °C under 5% CO2 for 16 h drug-to-light intervals. Control microplates not receiving a light treatment were kept in the dark in an incubator while light-treated microplates were irradiated under one of the following conditions: visible light (400-700 nm, 35.7 $mW \cdot cm^{-2}$) using a 190 W BenQ MS 510 overhead projector; or red light (625 nm, 32.3 $mW \cdot cm^{-2}$) from an LED array (PhotoDynamic Inc., Mount Uniacke, NS). Irradiation times using these two light sources were approximately 47 and 52 min, respectively, to yield total light doses of 100 $J \cdot cm^{-2}$. Both untreated and light-treated microplates were incubated for another 48 h before 10-μL aliquots of prewarmed Alamar Blue reagent (Life Technologies DAL 1025) were added to all sample wells and subsequently incubated for another 15-16 h. Cell viability was determined on the basis of the ability of the Alamar Blue redox indicator to be metabolically converted to a fluorescent dye only by live cells. Fluorescence was quantified with a Cytofluor 4000 fluorescence microplate reader with the excitation filter set at 530 ± 25 nm and emission filter set at 620 ± 40 nm. EC_{50} values for

cytotoxicity (dark) and photocytotoxicity (light) were calculated from sigmoidal fits of the dose–response curves using Graph Pad Prism 6.0 according to Eq 1, where where y_i and y_f are the initial and final fluorescence signal intensities. For cells growing in log phase and of the same passage number, EC_{50} values are generally reproducible to within ±25% in the submicromolar regime; ±10% below 10 μM; and ±5% above 10 μM. Photopherapeutic indices (PIs), a measure of the therapeutic window, were calculated from the ratio of dark to light EC_{50} values obtained from the dose-response curves. Selectivity factor (SF) was calculated from the ratio of dark EC_{50} values in CCD-1064Sk fibroblasts to that in SK-MEL-28 cells.

$$y = y_i + \frac{y_i - y_f}{1 + 10^{\left(log\ EC_{50} - x\right) \times (Hill\ slope)}}$$

Confocal Microscopy. Sterile glass-bottom Petri dishes (MatTek) were coated with 200 μL poly-$_L$-lysine (Ted Pella) in a laminar flow hood under standard aseptic conditions. After a 1 h incubation period at 37 °C, 5% CO2 in a water-jacketed incubator (Thermo Electron Corp., Forma Series II, Model 3110, HEPA class 100), the dishes were washed three times with sterile Dulbecco's phosphate buffered saline (DPBS 1X, Mediatech, 21-031-CV) containing 2.68 mM potassium chloride, 1.47 mM potassium phosphate monobasic, 0.137 M sodium chloride, and 8.10 mM sodium phosphate dibasic, pH 7.4, and were left to dry uncovered at room temperature for approximately 15 min. SK-MEL-28 malignant melanoma cells (ATCC HTB-72) and CCD-1064SK normal skin fibroblasts (ATCC CRL-2076) were then transferred in aliquots of 500 μL (approximately 100,000 cells) to the poly-$_L$-lysine-coated glass bottom Petri dishes and were allowed to adhere for 2 h in a 37 °C, 5% CO2 water-jacketed incubator. Metal compound (500 μL of a 50 μM solution in sterile PBS prewarmed to 37 °C) was added to sample dishes (destined to receive either a dark or light treatment), which were returned to the incubator for 15 min prior to further treatment; control dishes that did not contain the metal compound were also prepared. Light-treated samples were irradiated with visible light for 25 min from a 190 W BenQ MS 510 overhead projector (400−700 nm, power density = 33.1 mW cm^{-2}, total light dose ≈ 50 J cm^{-2}). Dark samples were covered with foil and placed in a drawer

for the same amount of time. Cells were then imaged at 15 min post-treatment using a Carl Zeiss LSM 510 laser scanning confocal microscope with a 60x oil objective lens. Excitation was delivered at 458/488 nm from an argon−krypton laser, and signals were acquired through a 475 nm long-pass filter. Pinhole diameters for all the treatments were 100 μm. The images were collected and analyzed using the Zeiss LSM Image Browser Version 4.2.0.121 software (Carl Zeiss Inc.).

DNA mobility-shift assays. DNA modification by compounds **1-5** was assessed according to a general plasmid DNA gel mobility shift assay with 30 μL total sample volumes in 0.5 mL microfuge tubes. Transformed pUC19 plasmid (3 μL, N 95% form I) was added to 15 μL of 5 mM Tris-HCl buffer supplemented with 50 mM NaCl (pH 7.5). Serial dilutions of the iridium compounds were prepared in ddH2O and added in 7.5 μL aliquots to the appropriate tubes to yield final iridium concentrations ranging from 1 to 100 μM. Then ddH2O (4.5 μL) was added to bring the final assay volumes to 30 μL. Control samples with no metal complex received 12 μL of water. Sample tubes were kept at 37 °C in the dark or irradiated. Light treatments employed visible light (14 J cm^{-2}) delivered from a Luzchem LZC-4X photoreactor over the course of 30 min. A softer light dose relative to that used in the cellular assays was required in order to see the topological changes to DNA before the DNA became too distorted to be imaged with the intercalating dye. After treatment, all samples (dark and light) were quenched by the addition of 6 μL gel loading buffer (0.025% bromophenol blue, 40% glycerol). Samples (11.8 μL) were loaded onto 1% agarose gels cast with 1 × TAE (40 mM Tris-acetate, 1 mM EDTA, pH 8.2) and electrophoresed for 30 min at 80 V cm^{-1} in 1 × TAE prior to staining for 30 min in an aqueous solution of 2 μg/mL ethidium bromide. The bands were visualized using the Gel Doc-It Imaging system (UVP) with Vision Works software, and further processed with the GNU Image Manipulation Program (GIMP).

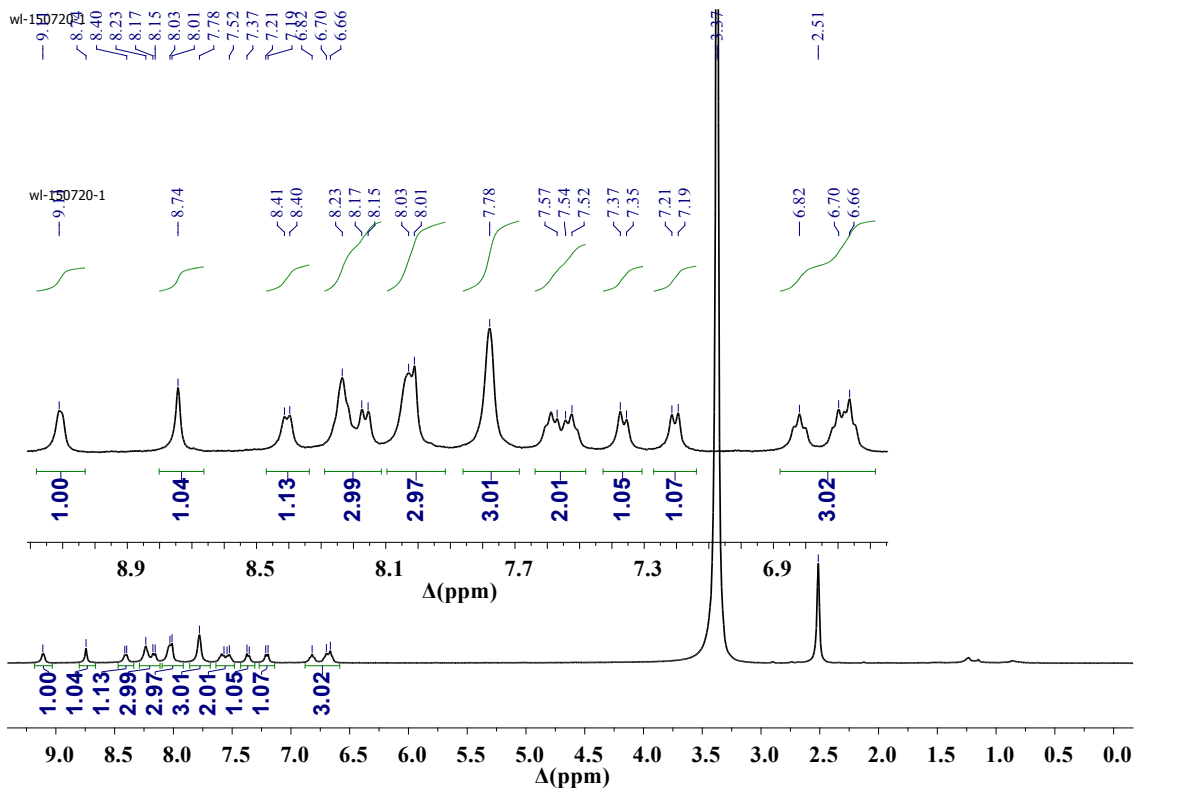

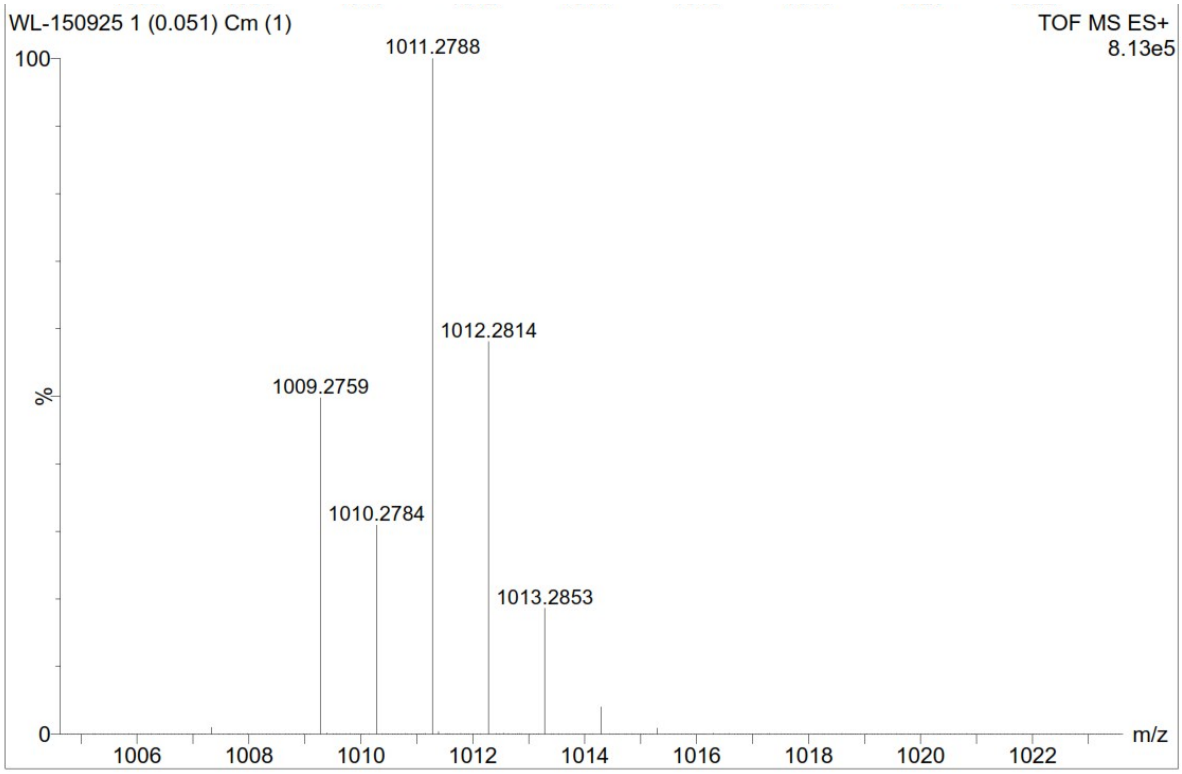

Figure S1. ^{1}H-NMR spectrum in d_6-DMSO and mass spectrum for complex **1.**

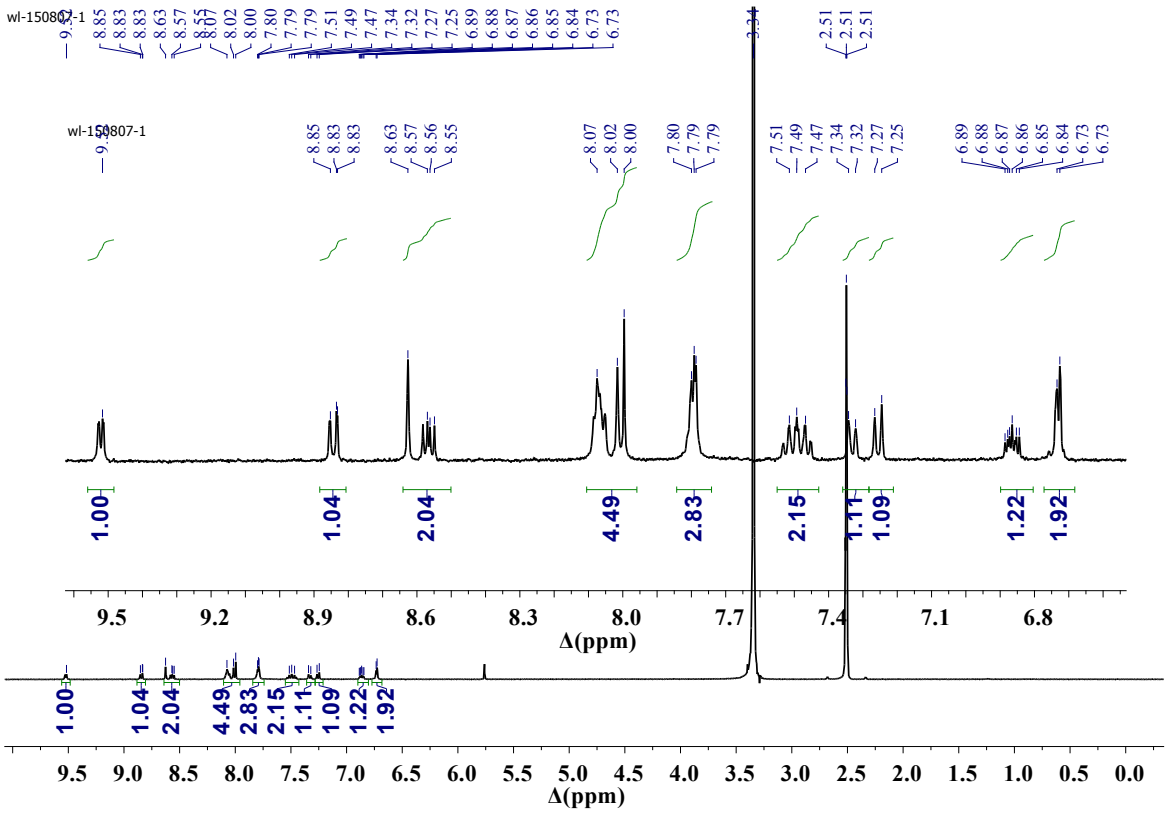

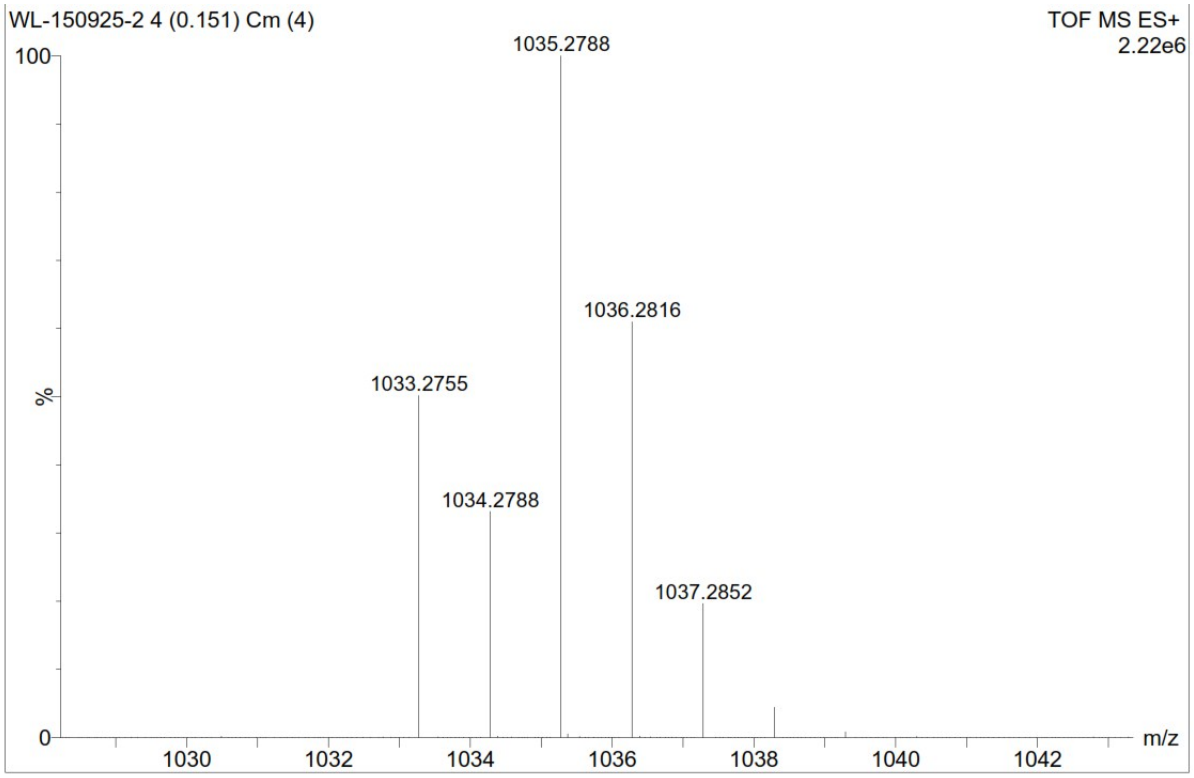

Figure S2. ^{1}H-NMR spectrum in d_6-DMSO and mass spectrum for complex **2.**

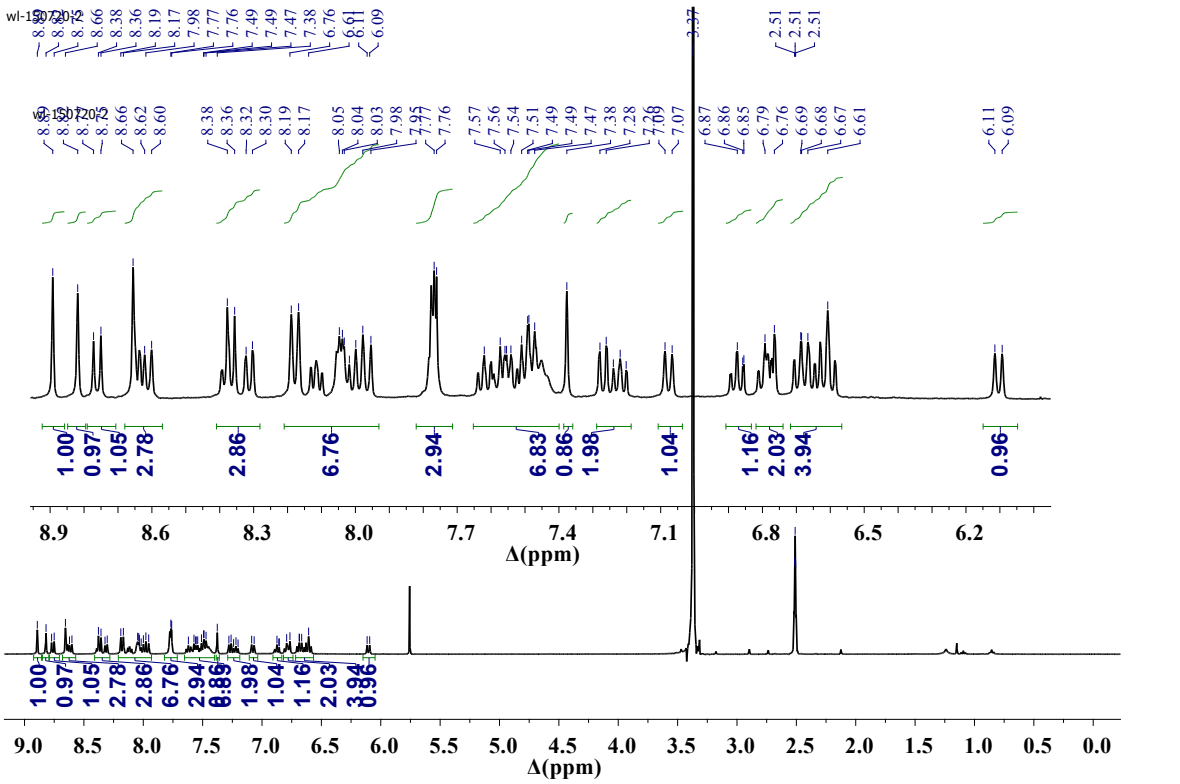

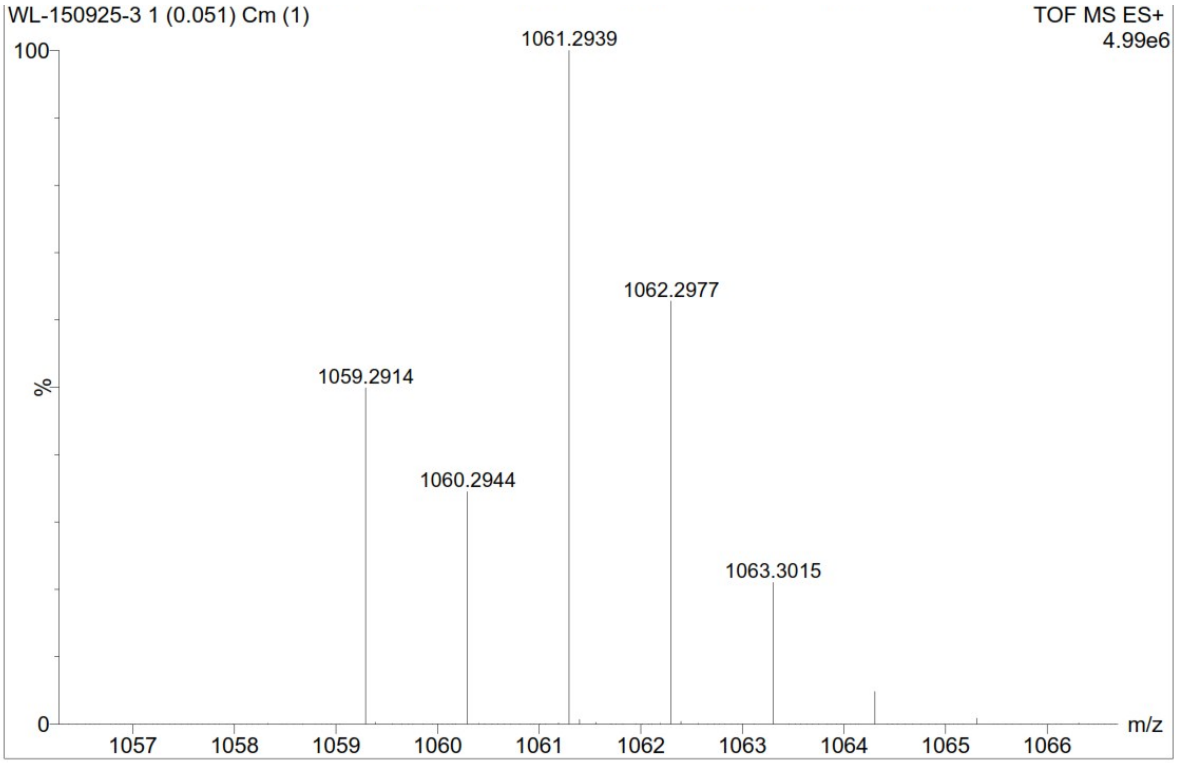

Figure S3. ^{1}H-NMR in d_6-DMSO and mass spectrum for complex **3.**

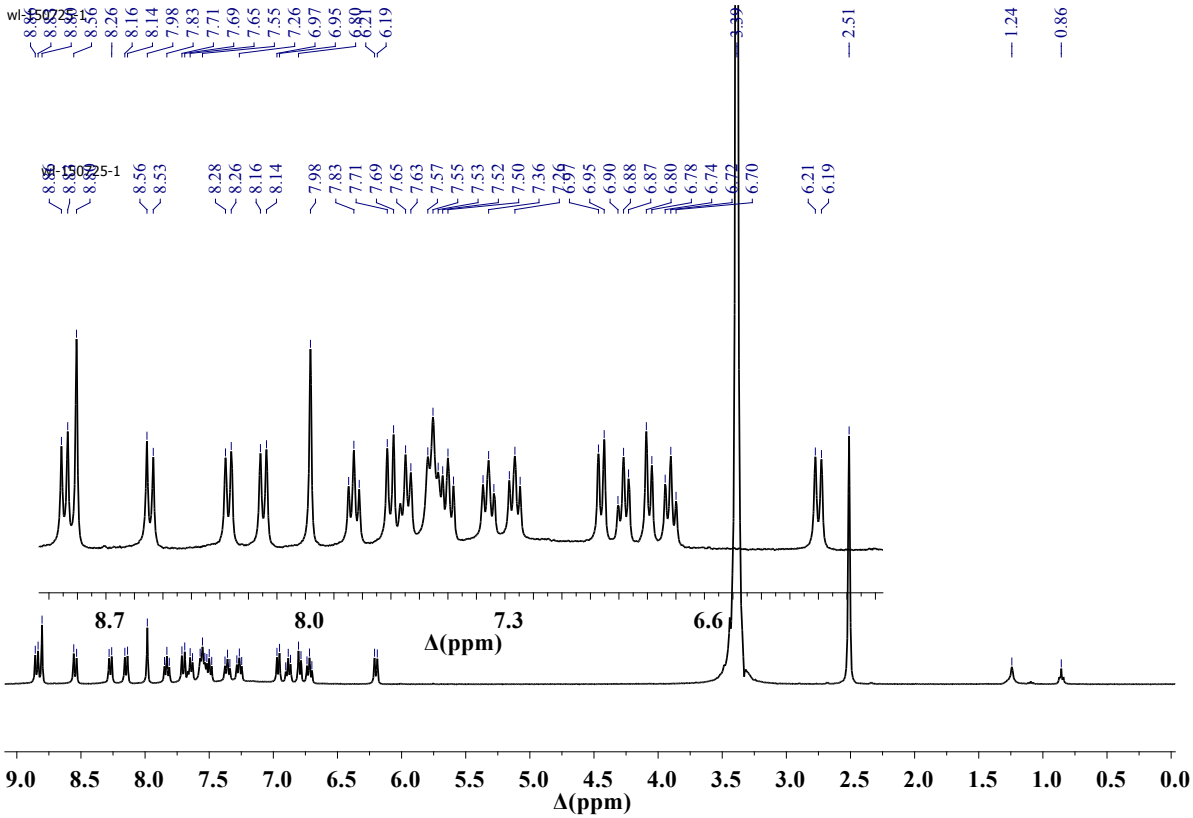

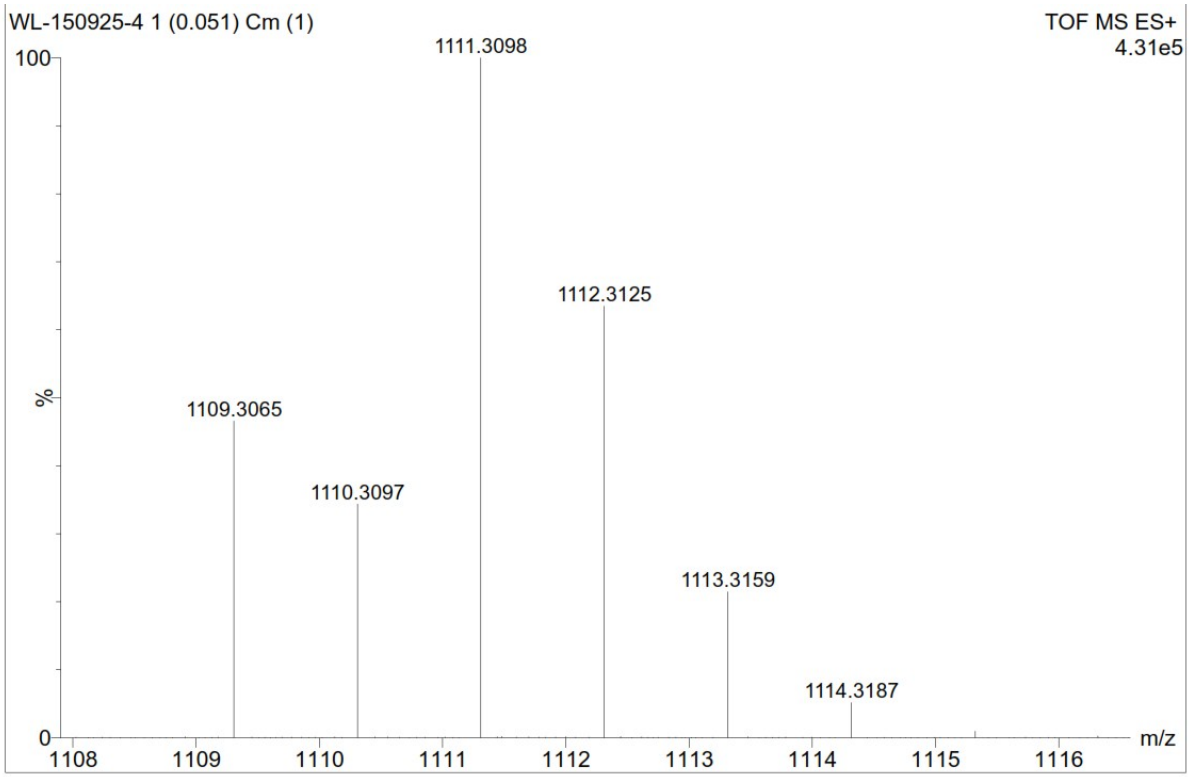

Figure S4. ^{1}H-NMR spectrum in d_6-DMSO and mass spectrum for complex **4.**

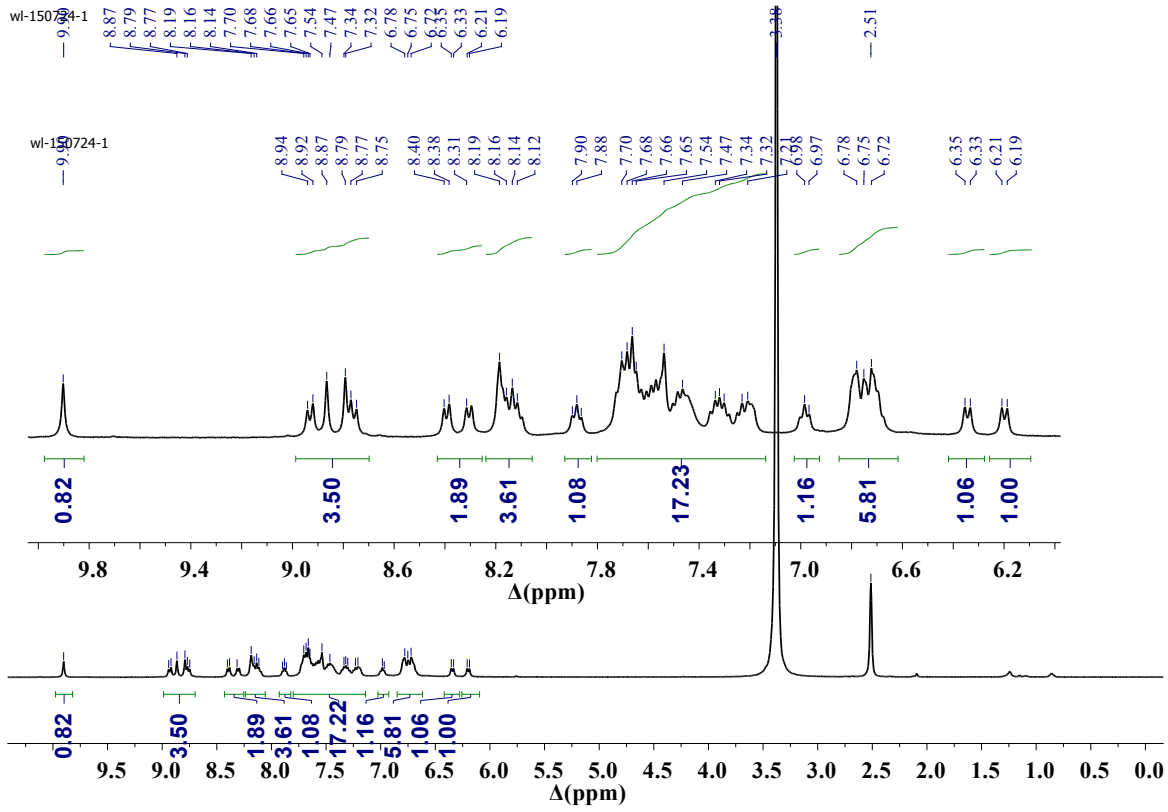

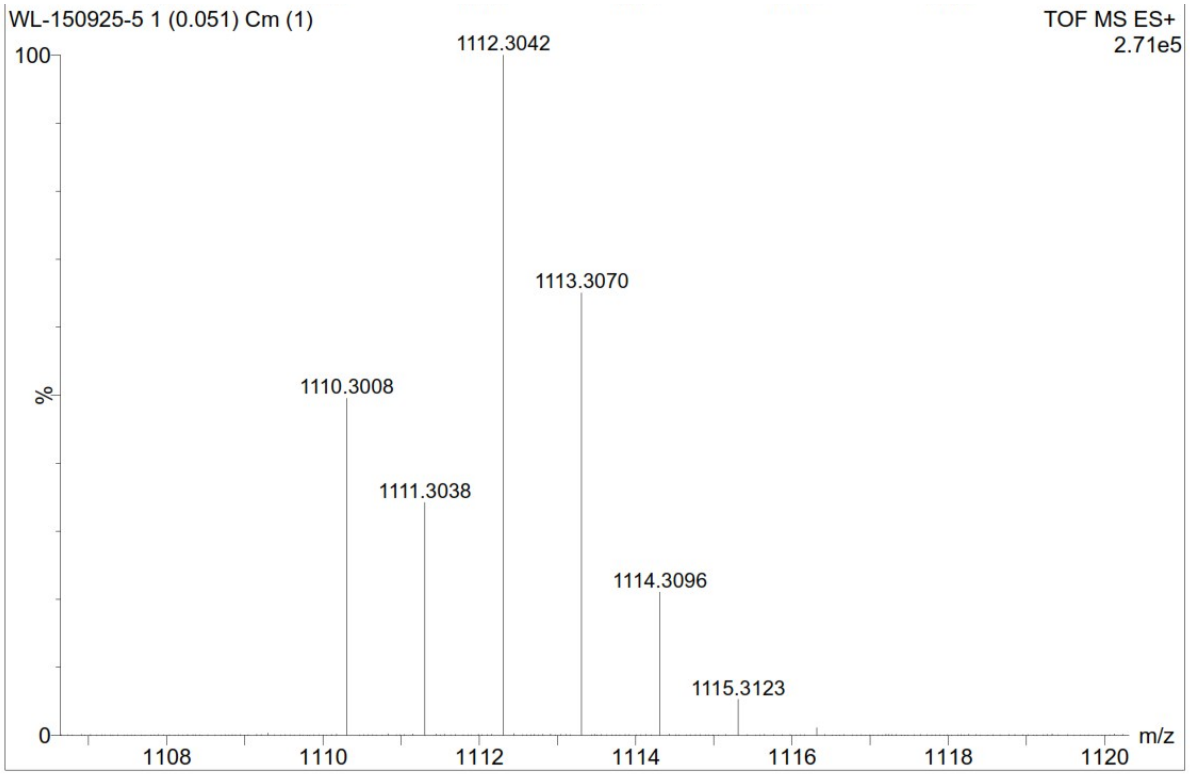

Figure S5. [1]H-NMR spectrum in d_6-DMSO and mass spectrum for complex **5.**

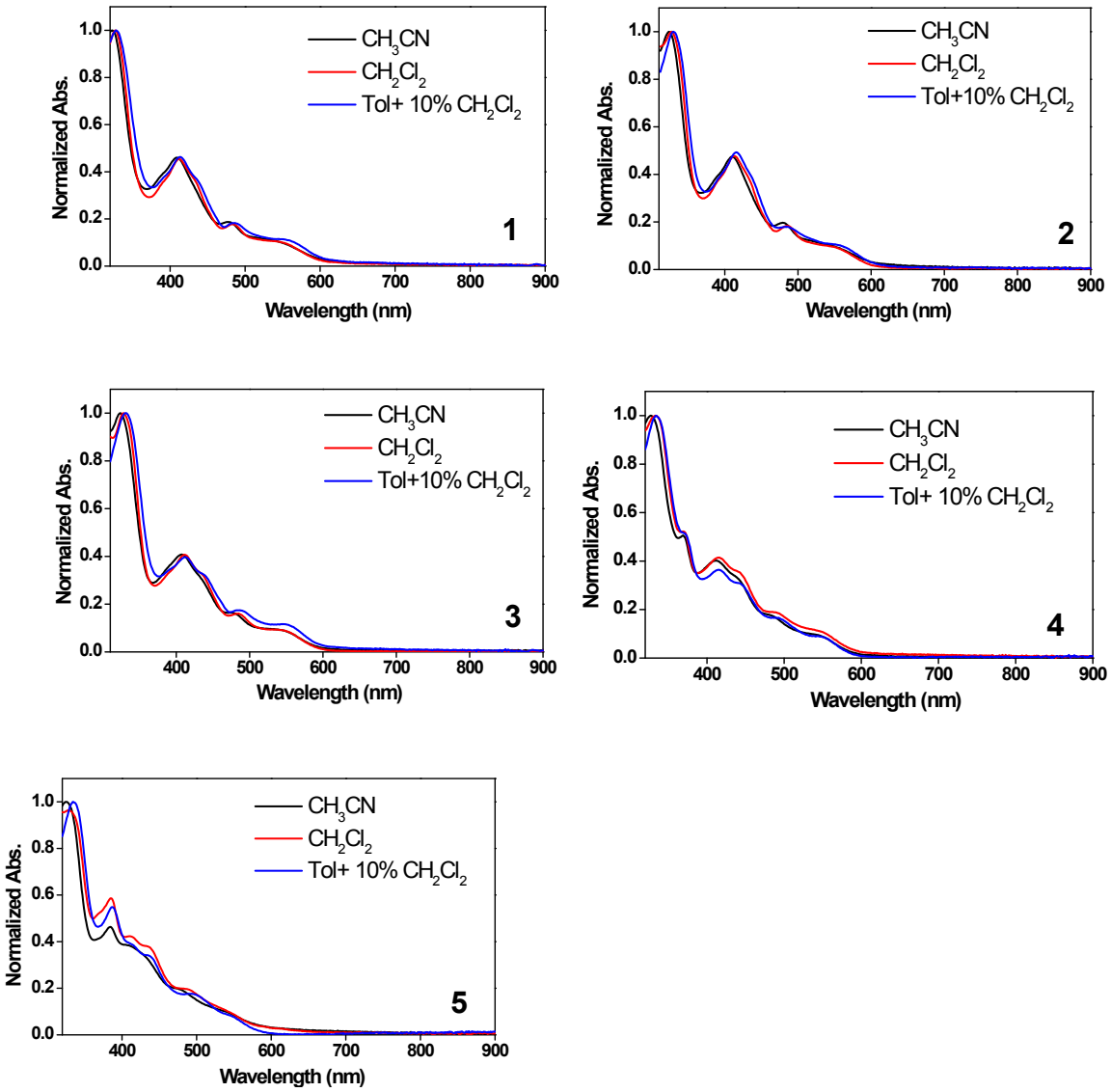

Figure S6. UV-vis absorption spectra of complexes **1-5** in different solvents.

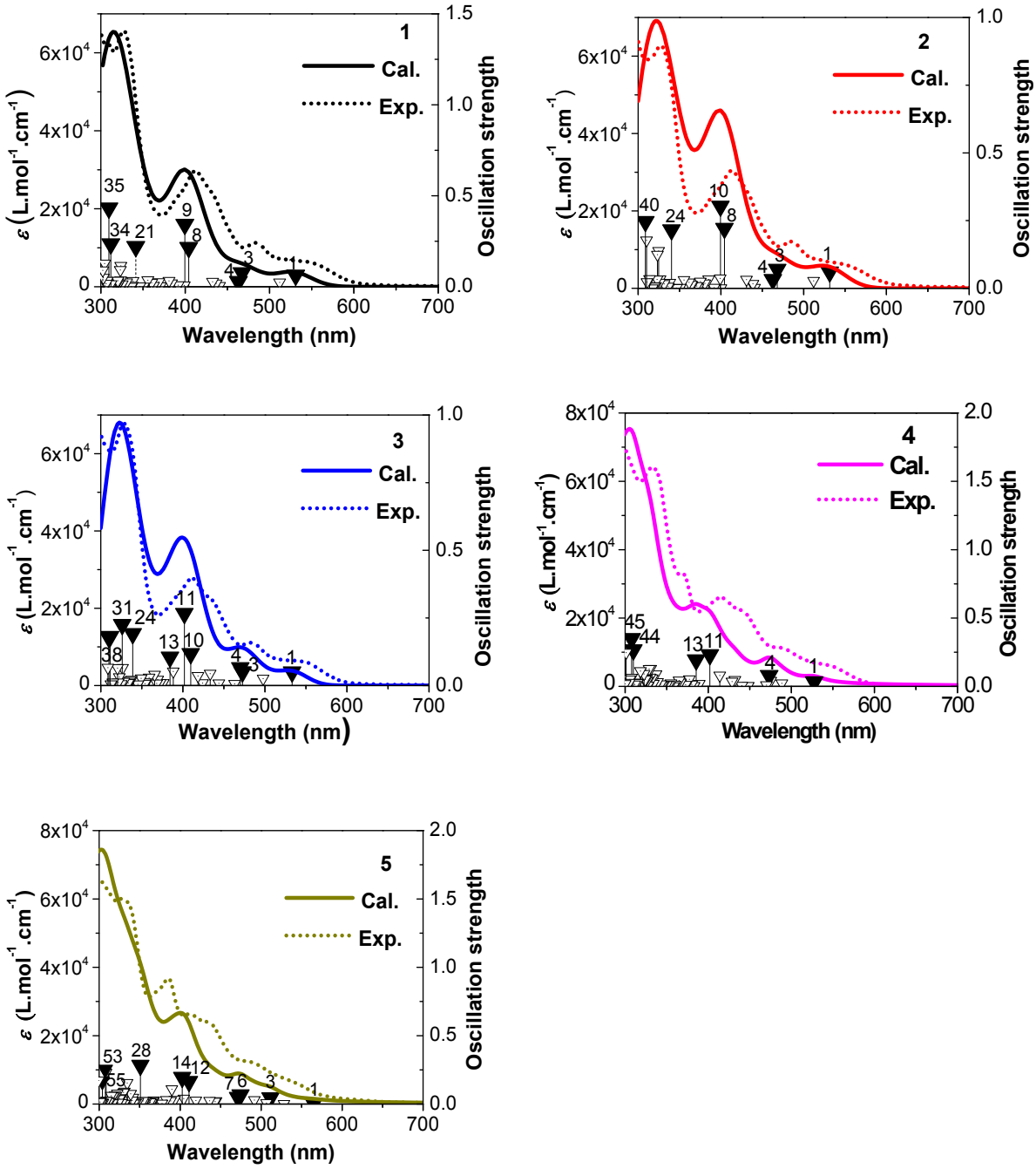

Figure S7. Comparison of the experimental and calculated UV-vis absorption spectra of complexes **1-5** in CH_2Cl_2.

Table S1. Natural transition orbitals (NTOs) representing the high-energy absorption bands below 350 nm.

		Hole	Electron		Hole	Electron
1	S_{21} 341 nm *f*=0.21	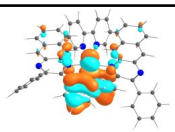	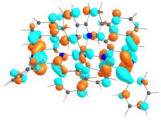	S_{34} 312 nm *f*=0.24	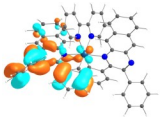 54%	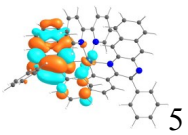 5 4%
	S_{35} 309 nm *f*=0.44	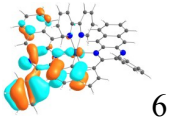 61 % 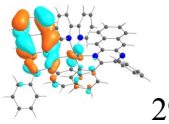 29 %	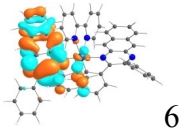 6 1% 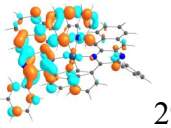 29 %		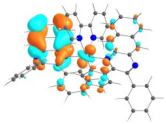 36%	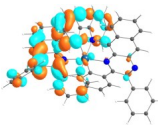 3 6%
2	S_{24} 340 nm *f*=0.22	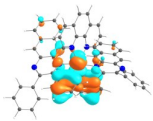	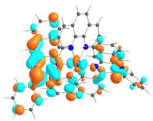	S_{40} 309 nm *f*=0.25	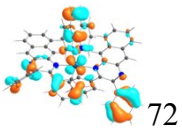 72 % 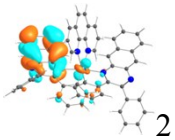 2 1%	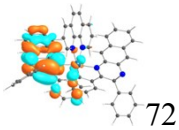 72 % 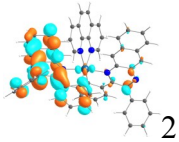 2 1%
3	S_{24} 339 nm *f*=0.19	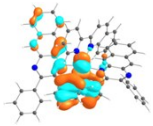	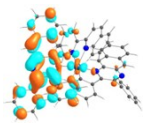	S_{31} 326 nm *f*=0.22	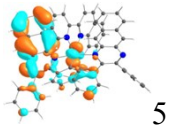 5 6% 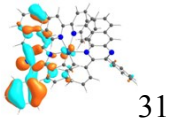 31 %	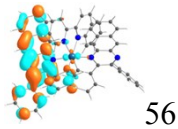 56 % 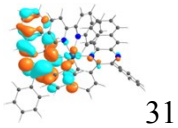 31 %

	S_{38} 311 nm *f*=0.18	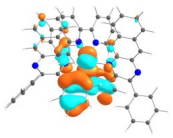	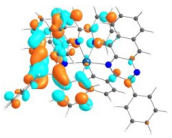	S_{39} 310 nm *f*=0.17	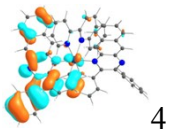 4 3% 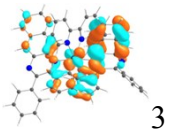 3 4%	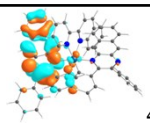 43 % 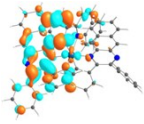 34 %
4	S_{34} 329 nm *f*=0.12	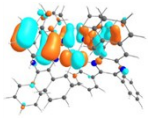 62 % 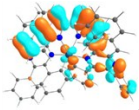 25%	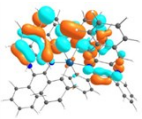 62 % 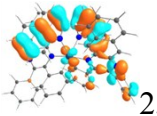 25 %	S_{40} 318 nm *f*=0.11	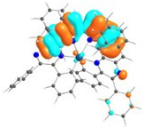	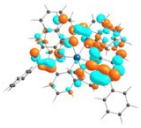
	S_{44} 309 nm *f*=0.26	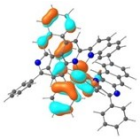 46% 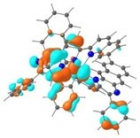 25%	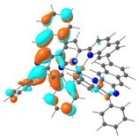 46% 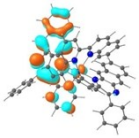 25%	S_{45} 307 nm *f*=0.35	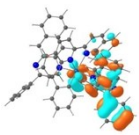 55% 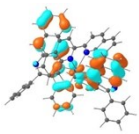 28%	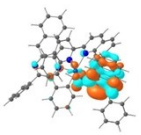 55% 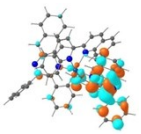 28%
5	S_{28} 351 nm *f*=0.28	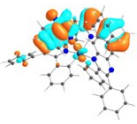	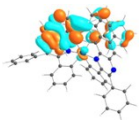	S_{53} 308 nm *f*=0.25	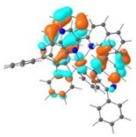 48% 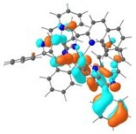 27%	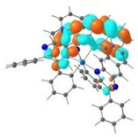 48% 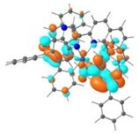 27%
	S_{55} 304 nm *f*=0.17		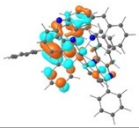			

	39% 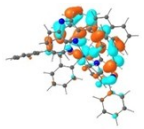 28%	39% 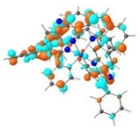 28%	

Table S2. Natural transition orbitals (NTOs) representing the low-energy absorption bands between 400 and 500 nm.

		Hole	Electron		Hole	Electron
1	S_3 468 nm *f*=0.13	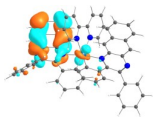	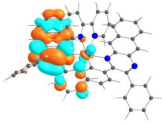	S_4 463 nm *f*=0.03	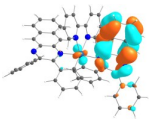	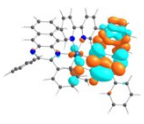
	S_8 404 nm *f*=0.22	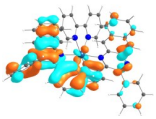	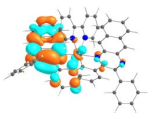	S_9 400 nm *f*=0.34	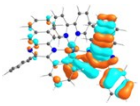	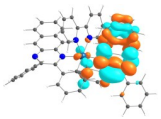
2	S_3 468 nm *f*=0.07	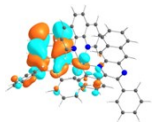	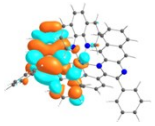	S_4 463 nm *f*=0.03	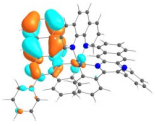	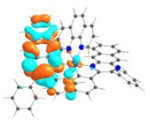
	S_8 404 nm *f*=0.22	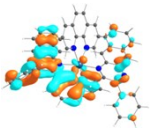	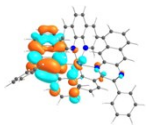	S_{10} 400 nm *f*=0.30	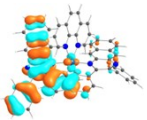	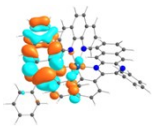
3	S_3 473 nm *f*=0.05	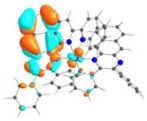	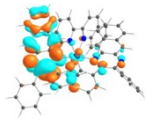	S_4 470 nm *f*=0.06	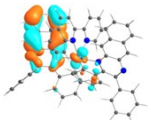	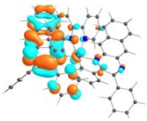
	S_{10} 410 nm *f*=0.11	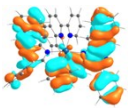 72 %	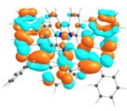 72 %	S_{11} 402 nm *f*=0.26	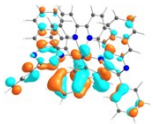 53%	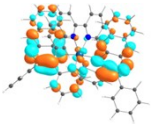 53%
		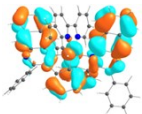 36 %	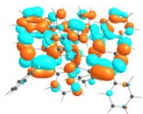 3 6%		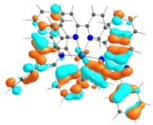 41%	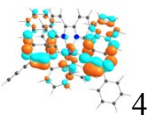 4 1%
	S_{13} 384 nm *f*=0.10	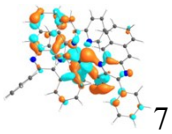 7 3%	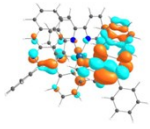 73%			
		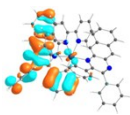 24 %	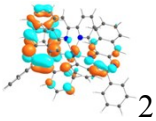 2 4%			

4	S_4 473 nm *f*=0.07	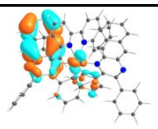	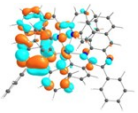	S_{11} 402 nm *f*=0.23	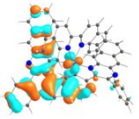 43%	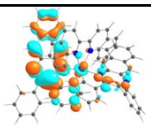 43%
					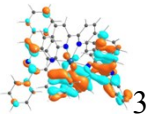 3 4%	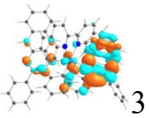 3 4%
	S_{13} 385 nm *f*=0.19	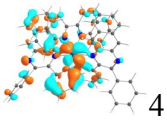 4 6%	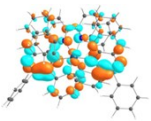 46%			
		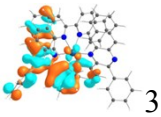 3 2%	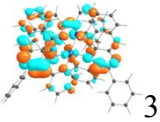 3 2%			
5	S_6 474 nm *f*=0.06	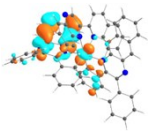	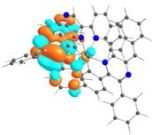	S_7 471 nm *f*=0.04	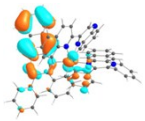	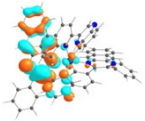
	S_{12} 411 nm *f*=0.16	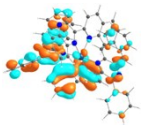	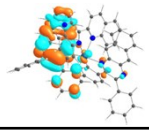	S_{14} 403 nm *f*=0.19	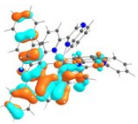	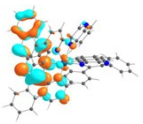

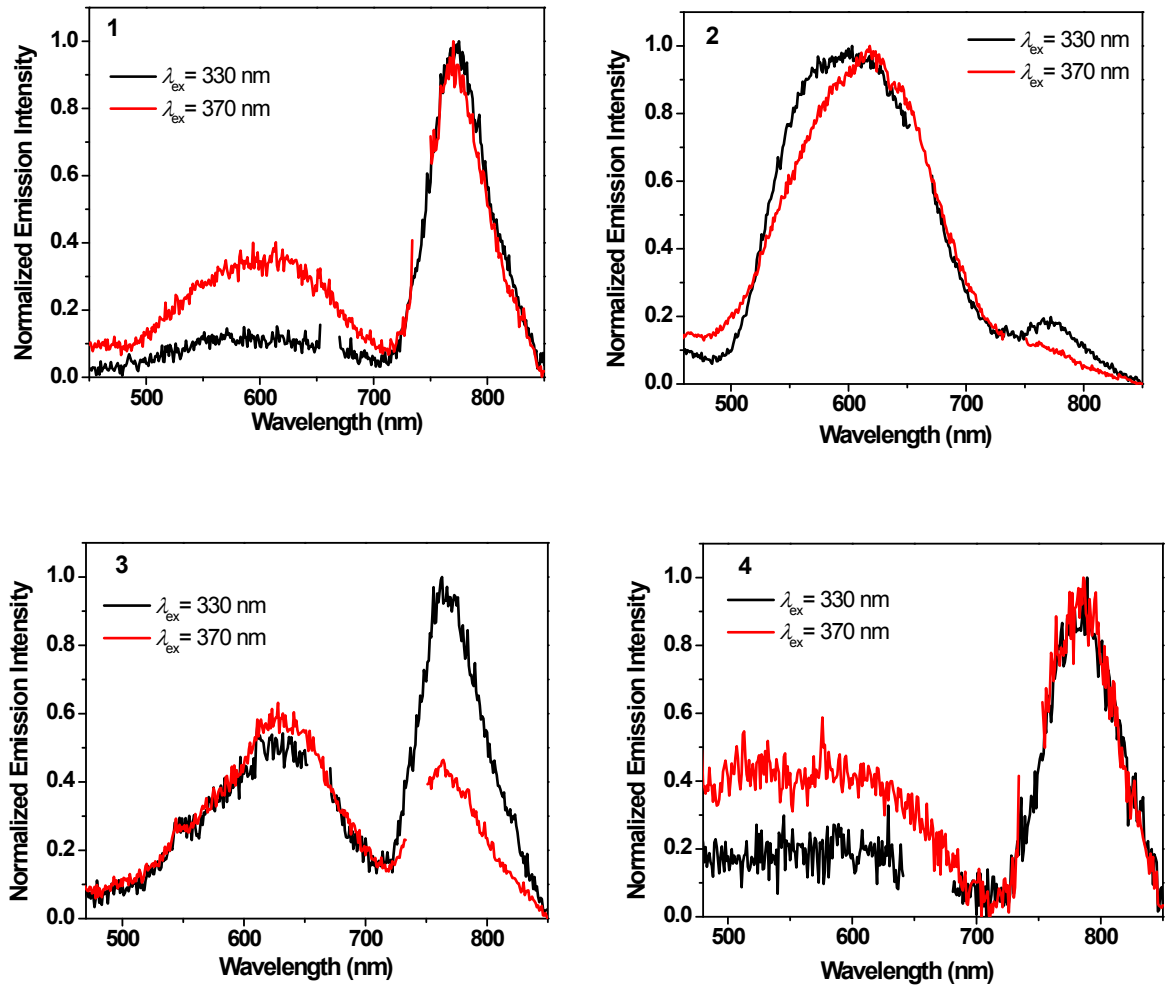

Figure S8. Normalized emission spectra of complexes **1-4** upon excitation at different wavelengths in CH_2Cl_2. The spectra were obtained on a Horiba Jobin Yvon FluoroMax-4 fluorometer/phosphorometer equipped with a Hamamatsu PMT R928.

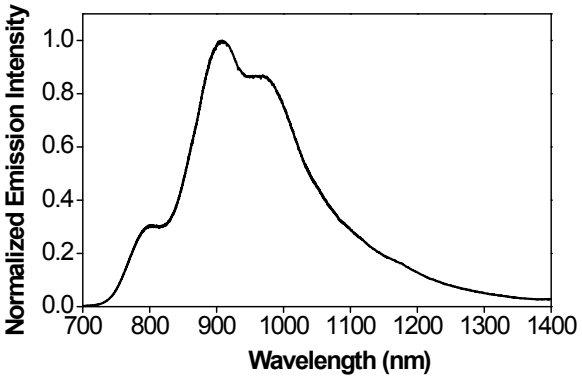

Figure S9. Normalized emission spectra of $[Ir(dpbq)_2Cl]_2$ dimer in deoxygenated CH_2Cl_2 at room temperature upon 473 nm excitation.

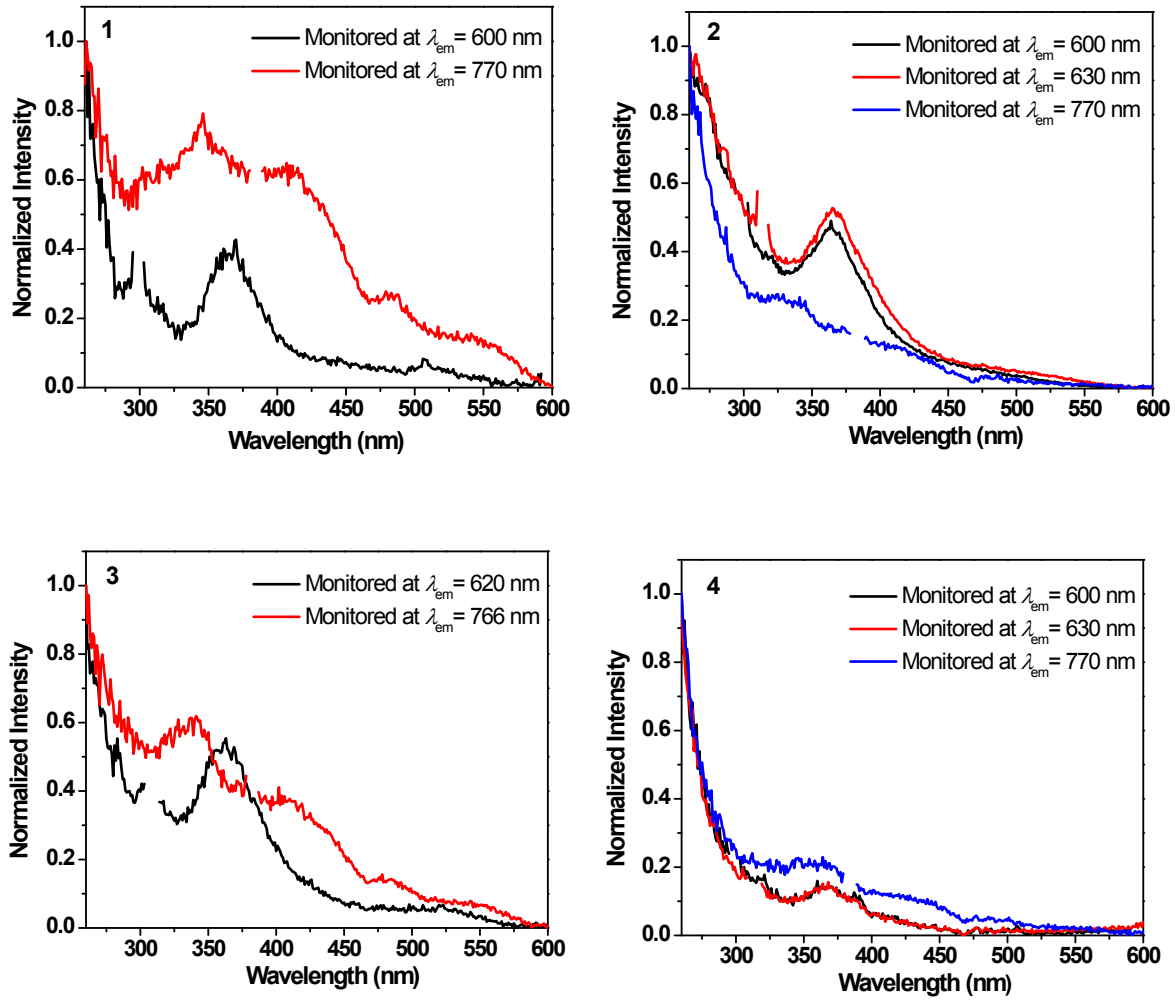

Figure S10. Normalized excitation spectra of complexes **1-4** monitored at different emission bands in CH_2Cl_2.

Table S3. Molecular orbitals (MOs) corresponding to the phosphorescence emitting states.

	Emission energy	Electron	Hole	Electron	Hole
1	770 nm	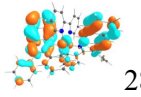 28%	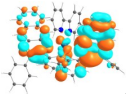 28%	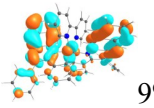 9%	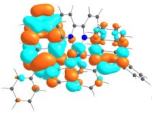 9%
		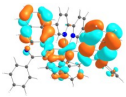 25%	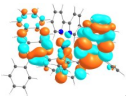 25%	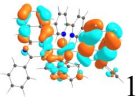 12%	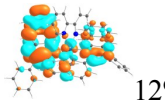 12%
		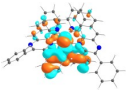 18 %	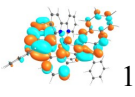 18%		
2	780 nm	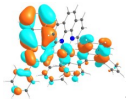 38%	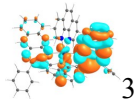 38%	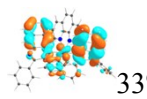 33%	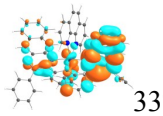 33%
		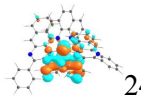 24%	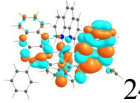 24%		
3	785 nm	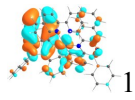 13%	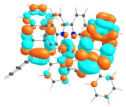 13%	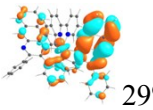 29%	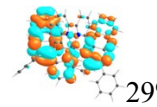 29%
		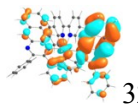 32%	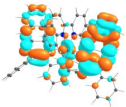 32%	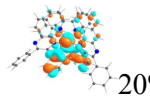 20%	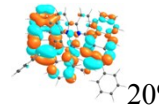 20%
		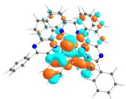 12%	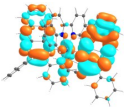 12%		
4	775 nm	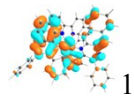 14%	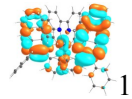 14%	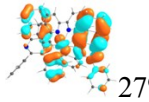 27%	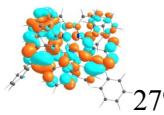 27%
		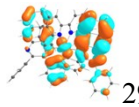 29%	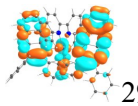 29%	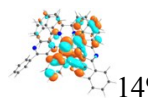 14%	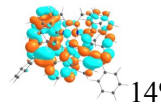 14%
		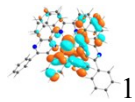 17%	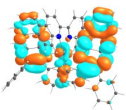 17%		
		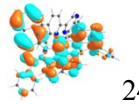 24%	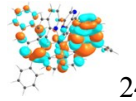 24%	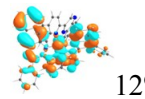 12%	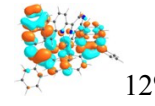 12%

5	790 nm	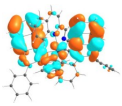	28%		28%	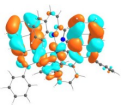	15%		15%
		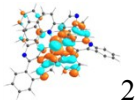	21%		21%				

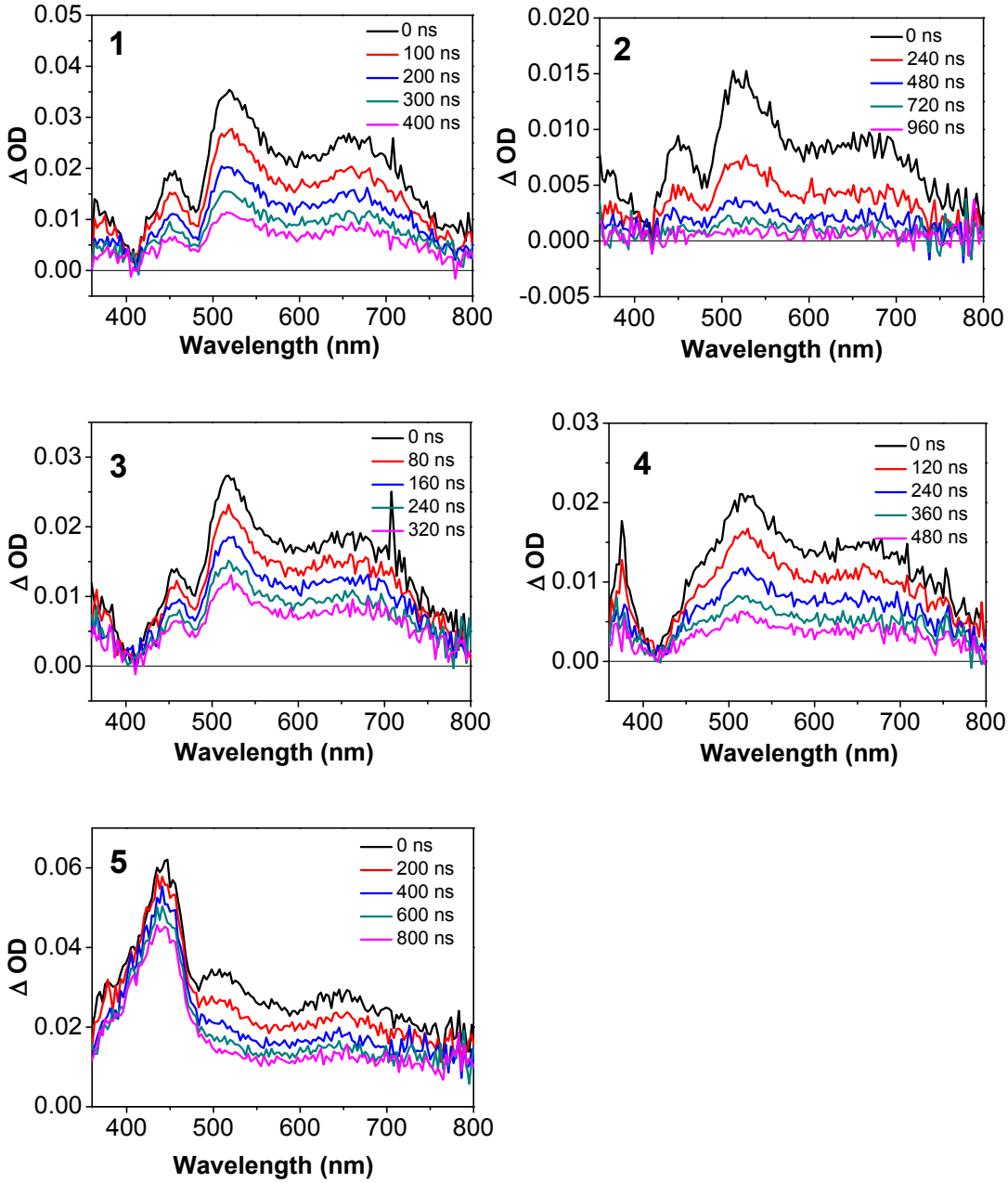

Figure S11. Time-resolved nanosecond TA spectra of **1-5** in acetonitrile solution (λ_{ex} = 355 nm, A_{355} = 0.4 in a 1-cm cuvette).

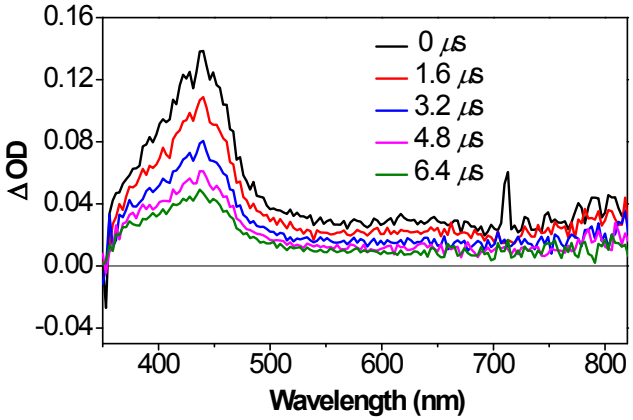

Figure S12. Time-resolved nanosecond TA spectra of quqo ligand in acetonitrile solution (λ_{ex} = 355 nm, A_{355} = 0.4 in a 1-cm cuvette)

Table S4. Comparison of EC_{50} values for CCD-1064Sk normal skin fibroblasts and SK-MEL-28 cancer cells dosed with complexes **1-5**.

	CCD-1064Sk	**SK-MEL-28**					
	Dark	**Dark**	**Vis PDT**		**Red PDT**		SF
	EC_{50} (μM)	EC_{50} (μM)	EC_{50} (μM)	PI	EC_{50} (μM)	PI	
1	13.5±0.83	17.9±2.27	0.252±0.017	71	1.71±0.12	10	0.8
2	11.4±0.47	0.34±0.03	0.015±0.001	23	0.16±0.05	2.1	34
3	9.11±0.64	0.23±0.03	0.018±0.004	13	0.15±0.01	1.5	40
4	2.27±0.12	2.92±0.68	0.123±0.006	24	2.11±0.21	1.4	0.8
5	3.63±0.45	3.27±0.14	0.012±0.001	273	0.20±0.01	16	1.1

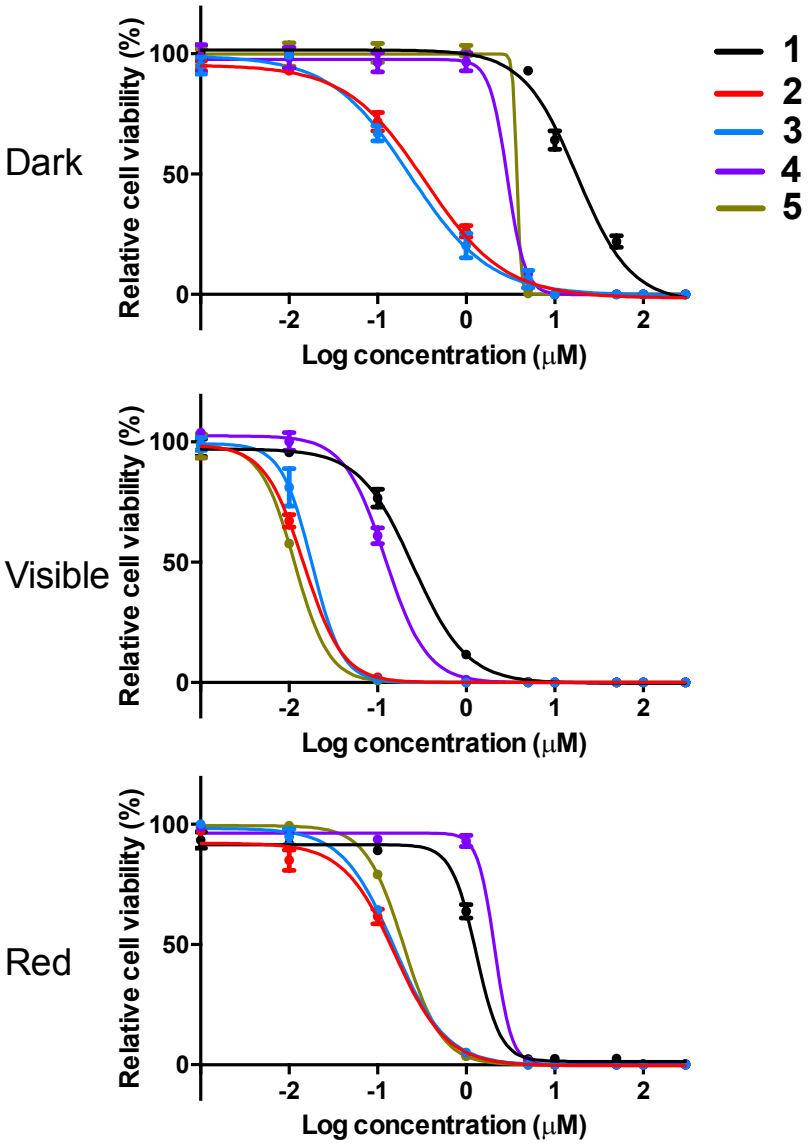

Figure S13. In vitro dose-response curves for complexes **1**, **2**, **3**, **4** and **5** in SK-MEL-28 cells in the dark and with visible or red (red) light activation.

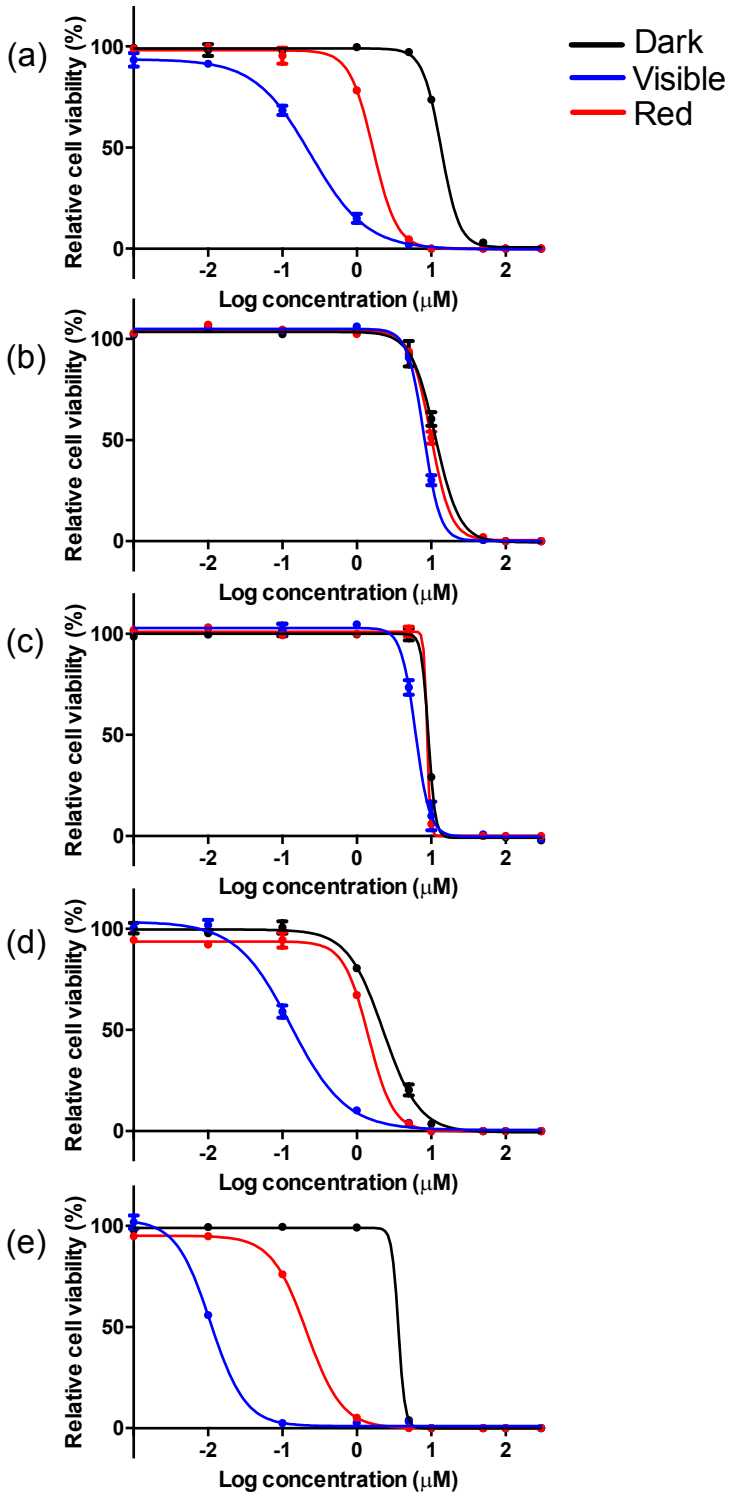

Figure S14. In vitro dose-response curves for complexes **1** (a), **2** (b), **3** (c), **4** (d) and **5** (e) in CCD-1064Sk normal fibroblasts in the dark (black) and with visible (blue) or red (red) light activation.